HHS Public Access

Author manuscript

Arch Biochem Biophys. Author manuscript; available in PMC 2015 December 21.

Published in final edited form as:

Arch Biochem Biophys. 2015 April 15; 572: 19–27. doi:10.1016/j.abb.2014.12.024.

Cellular localization of β-carotene 15,15′ oxygenase-1 (BCO1) and β-carotene 9′,10′ oxygenase-2 (BCO2) in rat liver and intestine

Shiva Raghuvanshi[a,1], **Vanessa Reed**[a,1], **William S. Blaner**[b], and **Earl H. Harrison**[a,*]

[a]Department of Human Sciences, The Ohio State University, Columbus, OH 43210, United States

[b]Department of Medicine, Columbia University, New York, NY 10032, United States

Abstract

The intestine and liver are crucial organs for vitamin A uptake and storage. Liver accounts for 70% of total body retinoid stores. Vitamin A deficiency (VAD) is a major micronutrient deficiency around the world. The provitamin A carotenoid, β-carotene, is a significant source of vitamin A in the diet. β-Carotene 15,15′ oxygenase-1 (BCO1) and β-carotene 9′,10′ oxygenase-2 (BCO2) are the two known carotenoid cleavage enzymes in humans. *BCO1* and *BCO2* are highly expressed in liver and intestine. Hepatocytes and hepatic stellate cells are two main cell types involved in the hepatic metabolism of retinoids. Stellate-like cells in the intestine also show ability to store vitamin A. Liver is also known to accumulate carotenoids, however, their uptake, retention and metabolism in specific liver and intestinal cell types is still unknown. Hence, we studied the cellular and subcellular expression and localization of BCO1 and BCO2 proteins in rat liver and intestine. We demonstrate that both BCO1 and BCO2 proteins are localized in hepatocytes and mucosal epithelium. We also show that BCO1 is also highly expressed in hepatic stellate cells (HSC) and portal endothelial cells in liver. At the subcellular level in liver, BCO1 is found in cytosol, while BCO2 is found in mitochondria. In intestine, immunohistochemistry showed strong BCO1 immunoreactivity in the duodenum, particularly in Brunner's glands. Both BCO1 and BCO2 showed diffuse presence along epithelia with strong immunoreactivity in endothelial cells and in certain epithelial cells which warrant further investigation as possible intestinal retinoid storage cells.

Keywords

Vitamin A; β-Carotene; β-Carotene 15,15′-oxygenase (BCO1); β-Carotene 9′,10′ oxygenase (BCO2); Hepatic stellate cells; Immunohistochemistry

*Corresponding author at: Department of Human Sciences, The Ohio State University, 314 Campbell Hall, 1787 Neil Avenue, Columbus, OH 43210, United States. Fax: +1 614 292 8880. Harrison.304@osu.edu (E.H. Harrison).

[1]These authors are listed alphabetically; both contributed equally to this work.

Introduction

Vitamin A and its derivatives play an essential role in vision, embryonic development, reproduction and cellular growth and differentiation [1–3]. Retinol derivatives such as *all-trans*- and 9-*cis*-retinoic acid serve as ligands for RAR and RXR nuclear hormone receptors that are proposed to control the expression of more than 500 genes [4,5]. Deficiency of this fat soluble vitamin leads to blindness, compromised immunity and even mortality when severe [6,7]. Since humans cannot synthesize vitamin A *de novo*, we consume it either as preformed vitamin A (retinyl esters) from animal sources or as provitamin A carotenoids, from fruits and vegetables. β-Carotene (β-C)[2] is the most potent of all carotenoids for provitamin A activity [8–10]. These carotenoids can also be absorbed and stored intact in animal tissues such as adipose tissue and liver [9,11]. β-Carotene 15,15′ oxygenase-1(BCO1) and β-carotene 9′,10′ oxygenase-2 (BCO2) are the only two mammalian enzymes known to oxidatively cleave carotenoids. BCO1 catalyzes central cleavage of provitamin A carotenoids at 15,15′ double bond to form two molecules of all-*trans*-retinal which can be further metabolized to vitamin A and its derivatives. In contrast to BCO1, BCO2 catalyzes eccentric cleavage of both provitamin and non-provitamin A carotenoids which results in the formation of apo-carotenoids such as β-apo- 10′ carotenal and β-ionone [12–17]. These two enzymes share 40% sequence homology and are both expressed in tissues such as small intestine, liver, kidney and lungs [14,17].

Carotenoids are absorbed along with other ingested nutrients in the small intestine. β-Carotene may first be metabolized to vitamin A and make its way to the liver as a retinyl ester, or it may be absorbed intact. If absorbed intact, β-carotene may either be stored or metabolized in the liver to vitamin A. In a well-nourished state, liver stores about 70% of the total vitamin A in the body. It is known that hepatocytes and hepatic stellate cells (HSC) are the two major cell types involved in the uptake and storage, respectively, of retinoids (retinol, retinyl esters) in liver [18]. Along with retinoid stores, liver has also been shown to accumulate significant amount of carotenoids under normal physiological conditions. *In vivo* and *in vitro* models have shown that both hepatocytes and hepatic stellate cells accumulate carotenoid [19–21]. Hepatic accumulation of β-carotene has been observed in both the *BCO1* and *BCO2*-deficient mice [22,23]. Hence, it is clear that liver plays a significant role in carotenoid metabolism either though central or eccentric cleavage pathways. The immunohistochemical study by Lindqvist and colleagues demonstrated BCO1 and BCO2 proteins are present in human hepatocytes [24,25]. However, a recent gene expression study has shown significantly higher *BCO1* mRNA levels in primary hepatic stellate cells (HSC) as compared to isolated primary hepatocytes in mice [20]. Additionally, while earlier studies have reported a cytoplasmic localization of BCO2 in cell, two recent studies demonstrate that BCO2 is a mitochondrial protein [22,26].

Greater understanding of the localization of carotenoid cleavage enzymes is needed to better understand the metabolism of carotenoids in liver and intestine. Hence, we studied the

[2]*Abbreviations used:* VAD, Vitamin A deficiency; BCO1, β-Carotene 15,15′ ’ oxygenase-1; BCO2, β-carotene 9′’,10′ ’ oxygenase-2; HSC, hepatic stellate cells; β-C, β-Carotene ; DMEM, modified Eagle’s medium; CHO, Chinese hamster ovary; ATCC, American Type Culture Collection; IHC, immunohistochemistry; PNS, post nuclear supernatant; PMS, post mitochondrial supernatant.

cellular and subcellular expression and localization of BCO1 and BCO2 proteins in rat liver and intestine. We demonstrate that both BCO1 and BCO2 proteins are localized in hepatocytes and mucosal epithelium. We also show that BCO1 is also highly expressed in hepatic stellate cells (HSC) and portal endothelial cells in liver. At the subcellular level in liver, BCO1 is found in cytosol, while BCO2 is found in mitochondria. In intestine, immunohistochemistry showed strong BCO1 immunoreactivity in the duodenum, particularly in Brunner's glands. Both BCO1 and BCO2 showed diffuse presence along epithelia with strong immunoreactivity in endothelial cells and in certain epithelial cells which warrant further investigation as possible intestinal retinoid storage cells.

Materials and methods

Cell lines

Rat hepatoma McArdle RH7777 (McA) cell line (ATCC, #CRL-1601) was maintained in Dulbecco's modified Eagle's medium (DMEM) supplemented with 10% fetal bovine serum (Sigma–Aldrich, St Louis, MO), 100 units penicillin and 100 μg streptomycin/ml (Invitrogen #15140), and 0.2 ml/100 ml Fungizone (Invitrogen #15290). Chinese hamster ovary (CHO) cells, stably transfected with mouse *BCO1* cDNA and referred as NY CHO cells in this study, were used as a positive control in assessing the specificity of the antibody for BCO1 protein. The non-transfected chinese hamster ovary cell line, obtained from American Type Culture Collection (ATCC, #CRL-10154), was referred to as ATCC CHO cells and was used as a negative control. NY CHO and ATCC CHO cells were maintained in basic medium, MEMα (+10% FBS, 100 units penicillin/streptomycin/ml, and 0.2 ml/100 ml Fungizone). All the cell lines were incubated at 37 °C with 5% CO_2 and 95% humidity. All chemicals were purchased from Invitrogen or as specified.

Antibodies

A rabbit polyclonal antibody against mouse BCO1 (IgG) referred to as "BCO1 antibody", was prepared as described [14]. A chicken anti BCO2 was prepared using a synthetic peptide unique to the C-terminus of human BCO2 (Genway biotech, San Diego, CA). A commercially-available rabbit antibody against human desmin (Novus Biological, Littleton, CO) was used as marker for hepatic stellate cells. Polyclonal rabbit anti-VDAC1 antibody was used as mitochondrial marker for immunostaining of Western blots.

Secondary antibodies used in immunohistochemistry (IHC) were; biotin–streptavidin-conjugated donkey anti-rabbit IgG and anti-chicken IgY (Jackson Immunoresearch, West Grove, PA). Peroxidase conjugated mouse anti-biotin IgG (Jackson Immunoresearch) was used as tertiary antibody. For Western blotting, secondary antibodies used were infrared dye conjugated, donkey anti-chicken and goat anti-rabbit (LI-COR biosciences, Lincoln, NE). For immunofluorescence, mitotracker dye (Invitrogen, Grand Island, NY) was used to stain mitochondria in McA cells and the secondary antibodies were conjugated to Alexa 488 including donkey anti-rabbit for BCO1 and donkey anti-chicken for BCO2. IHC also used a peroxidase conjugated mouse anti-biotin tertiary antibody (IgG) (Jackson Immunoresearch, #200-032-211).

Subcellular fractionation

Animal experiments were performed according to the guidelines of the Institutional Animal Care and Use Committee of The Ohio State University (Columbus, OH, USA). Livers were dissected from Sprague Dawley rats (body wt 260 g). Liver homogenate was prepared in 0.25 M sucrose (3 ml/gm) using Dounce and Omni tissue homogenizers and fractionated using differential centrifugation as described in [27]. The homogenate was centrifuged at 245×*g* for 10 min to separate nuclear fraction (pellet) from post nuclear supernatant (PNS). The PNS is subjected to centrifugation at 13,000×*g* for 13 min to give the mitochondrial (M) fraction in pellet form and post mitochondrial supernatant (PMS) fraction. This PMS fraction is again centrifuged at 138,000×*g* for 30 min which separated cell free cytosolic (S) supernatant fraction from microsomal (P) fraction. All steps were repeated three times and fractions were kept on ice at all times.

Western blot analysis

Fresh liver and intestine were removed from rat and homogenized with Radio-Immunoprecipitation Assay buffer (RIPA, Thermo Scientific, Rockford, IL) with protease inhibitor cocktail (PI, Roche Diagnostics, Indianapolis, IN) in a ratio of 1 g:5 ml for liver and 1 g:3 ml for intestine with an Omni Tissue Homogenizers (Kennesaw, GA). The small intestine was excised from the pyloric sphincter to the ileocecal valve and then further divided into eight equal sections. Mucosa was scraped from each intestinal segment.

Cultured cells were lysed with RIPA + PI. The collected lysate was centrifuged at 14,000 rcf at 4 °C for 15 min to get clear supernatant.

The total protein concentration of cells, tissue homogenates, or subcellular fractions was determined using the BCA protein assay (Thermo Scientific, Rockford, IL). Proteins were resolved by SDS–PAGE and transferred to nitrocellulose membranes (Millipore, Bedford, MA). After transfer, the blot was incubated with primary antibodies, rabbit anti-mouse BCO1 and chicken anti-human BCO2. Incubation was performed overnight at 4 °C on a rocker. Membranes were washed and incubated with infrared dye conjugated secondary antibodies, goat anti-rabbit and donkey anti-chicken for 30 min at room temperature. Blots were protected from direct light after secondary antibody incubation and observed with the Odyssey LI-COR Infrared Imaging System (LI-COR biosciences, Lincoln, NE).

Immunofluorescence staining

For further characterization of the antibody for BCO1, fluorescence immunostaining was used to visualize the expression of BCO1 in NY CHO cells. NY and ATCC CHO cells were seeded at a density of 1.5×10^5 cells/well on coverslips in 6-well plates and cultured overnight. Then, the cells were fixed with 4% (w/v) paraformaldehyde and permeabilized with 0.3% Triton X 100 (Fisher Scientific, Fair Lawn, NJ). After permeabilization, cells were washed and blocked with 5 mg/ml bovine serum albumin (BSA, Fischer Scientific) and 5% normal donkey serum (NDS, Jackson Immunoresearch) in PBS for 30 min to inhibit non-specific binding of primary and secondary antibodies. The primary antibody solution was applied, which comprised of rabbit polyclonal anti-mouse BCO1 antibody. Cells were incubated overnight at 4 °C. After incubating with primary IgG, cells were washed three

times with PBS and incubated with Alexa Fluor 488 conjugated donkey anti-rabbit which fluoresces green when excited at 499 nm. Prolong Gold antifade (Invitrogen, Carlsbad, CA, USA) mounting medium was applied and cells were visualized using Olympus IX71 epifluorescence microscope and Olympus cell sense software. Controls without primary antibodies were performed for both NY and ATCC CHO cells.

Confocal fluorescence microscopy

For the subcellular localization study, cells were plated on collagen coated coverslips (BD Biosciences). For mitochondria staining, live cells were treated with 400 nM mitotracker-red (Invitrogen, #M7512) for 15 min in incubator. After staining, cells were fixed in ice-cold methanol for 20 min and incubated with blocking buffer (5% BSA +2% NDS in PBS) for one hour. Primary antibody was used to localize endogenous BCO1 or BCO2 in cells, followed by 30 min incubation with Alexa 488 conjugated secondary antibody. After immunostaining, coverslips were mounted on glass slides using anti-fade mounting medium from Invitrogen. Images were captured by Olympus FV1000 spectral confocal microscope.

Immunohistochemistry

Immunohistochemical staining was performed to determine the localization of BCO1 and BCO2 proteins in rat liver and intestinal cells. Formalin-fixed, paraffin-embedded rat liver and intestinal sections of 3–5 μm were prepared by Veterinary Histology Laboratory Services, The Ohio State University (Columbus, OH, USA). Before proceeding with staining, paraffin sections were first deparaffinized in xylene and rehydrated in graded ethanol. Sections were treated with 3% hydrogen peroxide to block endogenous peroxidase activity and blocked with 3% BSA and 1.28% NDS in PBS (pH 7.4). After blocking, sections were incubated with primary antibodies: rabbit anti-mouse BCO1, chicken anti-BCO2, goat anti-human desmin, and rabbit anti-villin. Tissues were then incubated with biotin-SP conjugated secondary antibodies: donkey anti-rabbit; donkey anti-chicken IgY, and donkey anti-goat. An anti-biotin conjugated horseradish peroxidase (HRP) tertiary antibody was used followed by diaminobenzidine (DAB, Dako, Carpinteria, CA) and counterstained with Gill's Hematoxylin (Fisher Scientific, Fair Lawn, NJ). Controls were performed without primary antibodies for all the antibodies. Sections of rat liver and intestinal tissue were examined using Olympus BX51 light microscope with 10×, 20×, 40× and 60× objective. DP Manager Software was used to digitally record images.

Results

Characterization of antibodies

The specificity of the antibodies towards BCO1 and BCO2 proteins was tested using immunofluorescence. CHO cells stably transfected with *BCO1* cDNA were positively stained by antibody to BCO1 (Fig. 1, panel D) but not with antibody to BCO2 (Fig. 1, panel C). No staining was observed in non-transfected normal CHO cells for either BCO1 (Fig. 1, panel A) or BCO2 (Fig. 1, panel B). Antibody specificity was further verified with Western blot (Fig. 1, gel image on right). The anti-BCO1 antibody reacts specifically with a protein band at the correct molecular weight (~63 kDa) in positive control cells (Fig. 1, right, lane: BCO1) and whole rat liver homogenate (Fig. 1, right, lane: LIVER). Similarly, anti-BCO2

antibody reacted with an approximately ~60 kDa protein in whole rat liver (Fig. 1, right, lane: LIVER) and shows no reactivity with lysate of *BCO1* cDNA transfected cell line (Fig. 1, right, lane: BCO1). Neither antibody reacted with lysate from negative control cells (Fig. 1, right, lane: ATCC).

The specificity of the anti-desmin antibody (marker for quiescent hepatic stellate cells) was also tested by Western blot. A single band for desmin protein was detected at the predicted molecular weight of 52 kDa in rat liver. No labeling was observed in either NY CHO or ATCC CHO cells (data not shown).

Immunolocalization of BCO1 and BCO2 protein in liver

We first studied the localization of BCO1 and BCO2 in cells in the portal triad and central vein areas of the liver (Fig. 2). Comparison of serial tissue sections treated with anti-BCO1 (Fig. 2A) and anti-BCO2 (Fig. 2B) and controls without primary antibodies (Fig. 2C) indicate strong BCO1 labeling in the endothelial cells lining the portal vein (Fig. 2A, black arrows) and hepatic artery (Fig. 2A, red arrow). The staining of the endothelial cells was not observed for BCO2. However neither BCO1 nor BCO2 antibody showed labeling of endothelial cells lining the central vein (Fig. 2D–E, arrows). Fig. 3 shows BCO1 expression in endothelial cells in portal triads at higher magnification. In parenchyma, the BCO2 protein expression was limited in hepatocytes (Fig. 4, right panels). However, BCO1 protein was expressed in parenchymal and non-parenchymal, lipid-containing, stellate cells (Fig. 4, left panels).

We observed strong immunoreactivity of anti-BCO1 antibody in lipid containing hepatic stellate cells (HSC), also called lipocytes because of their characteristic feature of having lipid droplets in its cytoplasmic processes (Fig. 5, insets). BCO1 was also observed to be expressed in hepatocytes, with uniform labeling of the cytoplasm (Fig. 5). To confirm the BCO1 expression in HSC, we compared the anti-BCO1 labeling with the stellate cell marker, desmin, in serial sections (Fig. 6). We observed that the stellate cells stained for desmin (Fig. 6, right panels) were also strongly stained by anti-BCO1 antibody (Fig. 6, left panels).

Subcellular localization of BCO1 and BCO2 in liver

We studied the subcellular localization of BCO1 and BCO2 proteins using liver fractions. Cell fractions were prepared from liver tissue by differential centrifugation and Western blots were performed. We probed the cell fractions with both anti-BCO1 and anti-BCO2 antibodies (Fig. 7). The cytosolic fraction was found to be enriched in BCO1 (Fig. 7, right, lane: S) and the mitochondrial fraction was found to be enriched in BCO2 protein (Fig. 7, left, lane: M). In order to test the purity of the mitochondrial fraction, we probed the fractions with anti-VDAC1, a mitochondrial marker. The labeling pattern of VDAC1 was similar to BCO2 protein in mitochondrial fraction (Fig. 7, lower left, lane: M). There small bands of both BCO2 and VDAC1 in the nuclear fraction (Fig. 7, left, lane: N) are likely due to slight contamination of mitochondria in this fraction.

The subcellular localization of BCO2 in mitochondria was verified by double-immunofluorescence staining of McA cells for endogenous BCO2 protein using anti-BCO2 antibody and mitotracker dye (Fig. 8). The merged image for BCO2 and mitotracker dye shows complete co-localization (Fig. 8, panel-Merge).

Immunolocalization of BCO1 and BCO2 protein in intestine

In addition to liver, intestinal sections were also examined for presence of carotenoid cleavage enzymes. BCO1 immunoreactivity showed a gradient in the 3 sections with strongest presence in the duodenum which tapered to lower presence in the jejunum and ileum (Fig. 9). Immunoreactivity was so strong in the duodenum, that the antibody was diluted to twice that used for the jejunum and ileum. BCO1 was present in the mucosa, submucosa and muscularis. Immunoreactivity was stronger in the villi than the crypts. Strongest presence occurred in Brunner's glands of the duodenum and endothelial cells. Localization of BCO2 in intestine was similar to that of BCO1 in that BCO2 also revealed strongest immunoreactivity in the duodenum with lesser immunoreactivity in the jejunum and ileum (Fig. 10). However BCO2 was not found in duodenal Brunner's gland cells. For both BCO1 and BCO2 there are also strongly immunoreactive, small cells along the villi that may be specific epithelial cells (Fig. 11). A greater presence was observed in villi than in crypts. A notable difference between BCO1 and BCO2 is stronger immunoreactivity for BCO2 in cells that are dispersed throughout the epithelial cells of the villi and Peyer's patches (Fig. 11). Further investigation is warranted to identify these cells.

Discussion

Hepatic retinoid stores account for approximately 70% of the total body vitamin A. It is also proposed that 8–12% of total body β-C is taken up by the liver [28]. Retinoids taken up by the liver are primarily metabolized in hepatocytes and stored as retinyl esters in hepatic stellate cells (HSC) [18]. In this study, we have demonstrated that carotenoid cleavage enzymes – BCO1 and BCO2 – are uniformly expressed in hepatocytes. This agrees well with earlier studies showing BCO1 and BCO2 localization in hepatocytes [24,25]. The expression of BCO1 in hepatocytes clearly demonstrates a tissue specific synthesis of vitamin A from the central cleavage of provitamin A carotenoids, such as β-carotene. The observed expression of BCO2 in hepatocytes is in agreement with a recent study that also demonstrated *BCO2* mRNA expression in isolated primary hepatocytes [20]. BCO2 protein in hepatocytes may be involved in the synthesis of vitamin A via an alternate pathway, one which was suggested earlier [25]. As BCO2 has broad substrate specificity, its role might also be cleaving non-provitamin A carotenoids, such as xanthophylls, taken up by the liver.

Hepatic stellate cells (HSC) are known to be the cellular site for hepatic retinoid storage. An *in vitro* model of HSC, GRX cells, have been shown to accumulate carotenoids such as β-carotene and lycopene and also are active in the conversion of β-carotene to retinoids [19,21]. We have observed that along with hepatocytes, BCO1 protein is highly enriched in the lipid containing HSC. Our findings are consistent with recent reports. *BCO1* mRNA expression was about 4-fold higher in isolated HSC as compared to hepatocytes [20,29]. Thus, the observed expression of BCO1 in HSCs directly implies a carotenoid metabolic

pathway in these non-parenchymal cells. It is probable that the central cleavage pathway may initiate cell specific transcriptionally active retinoid production. It has been recently shown that *BCO1* mRNA expression increases 20-fold in the wake of liver wound healing [29], demonstrating the importance of BCO1 in synthesizing central cleavage products from pro-vitamin A carotenoids in the liver.

Even on a vitamin A sufficient diet, BCO1 knockout mice demonstrated an increased accumulation of β-carotene as well as increased triglyceride levels in liver and developed liver steatosis over a period of time. Also there was an increased gene expression of PPARγ in HSC, but not in hepatocytes, of $BCO1^{-/-}$ compared to a wild type mice [23]. Thus, the observed expression of BCO1 protein in HSC implies a significant role for BCO1 in retinoid as well as in lipid homeostasis in the liver.

LRAT is the enzyme involved in the esterification of retinol to retinyl esters, the storage form of retinoids in HSC and the enzyme is highly enriched in HSC. There is also evidence regarding a possible function of endothelial cells in retinoid metabolism. A study by the Matsuura group has localized LRAT in portal and sinusoidal endothelial cells in rodent liver [30]. Interestingly, we have also observed immunolocalization of BCO1 protein in endothelial cells of portal vein and hepatic arteries. The BCO1 expression in our study was limited to endothelial cells of portal triads, no staining was observed in either sinusoidal or endothelial cells lining the central vein. *BCO1* mRNA has also been observed in endothelial cells of glomeruli and tubuli in the chicken kidney [31]. Endothelial cells have not been studied extensively in respect to the vitamin A metabolism, however it is known that endothelial cells work in coordination with HSC to regulate the blood flow through hepatic sinusoids [32]. The significance of BCO1 localization in endothelial cells is presently unclear.

At cellular level, BCO1 and BCO2, both are expressed in hepatocytes whereas BCO1 is also expressed in HSC and portal endothelial cells in rat liver. The previous study on BCO1 immunolocalization was performed on human tissues showing BCO1 expression only in liver hepatocytes [24]. The reason for this may be due to the use of lower magnification. Moreover, no markers were used in previous study to distinguish the labeling between parenchymal and non-parenchymal cells.

Two recent publications suggested the mitochondrial subcellular localization of BCO2 enzyme based on the localization of an expressed tagged protein and endogenous BCO2 in mouse liver [22,26]. Hence we examined the subcellular expression of endogenous BCO1 and BCO2 proteins in liver cellular fractions (post nuclear supernatant (PNS), mitochondrial (M), microsomal (P) and cytosolic (S)) and in rat hepatoma McA cells. Our data showing that endogenous BCO2 is a mitochondrial protein in rat liver is fully consistent with these recent reports of von Lintig and colleagues [22,26]. Confocal microscopy studies reveal that BCO2 co-localizes with mitochondria in McA cells. The finding that BCO2 protein is associated with mitochondria suggests that eccentric carotenoid cleavage products may have some mitochondrial specific functions as recently proposed [22,26].

There is increased evidence regarding overlapping expression of *BCO1* and *BCO2* mRNA with carotenoid accumulating tissues. A recent study reported a significant accumulation of dietary β-carotene in hepatocytes and HSCs in liver [20]. Thus, the results of the present study showing that BCO1 and BCO2 proteins are localized in hepatocytes and the specific expression of BCO1 in hepatic stellate and endothelial cells, indicate that liver is also an important site in the metabolism of dietary β-carotene as well as the major vitamin A storage site. The precise function of BCO1 in hepatic stellate cells and endothelial cells remains to be elucidated.

As in a previous study [24] of the small intestine in humans, BCO1 was found in epithelial cells along length of the small intestine, particularly in the villi. The present study extends these findings by demonstrating BCO1 expression in endothelial cells as well as cells in the submucosa and muscularis. Endothelial cells need retinoic acid for proliferation and vascular remodeling [33]. BCO1 therefore, may provide an important precursor to retinoic acid for these cells. Immunoreactivity of the muscularis is not altogether surprising since BCO1 is known to occur in skeletal muscle [24]. There were also cells in the mucosa with strong immunoreactivity that warrant further investigation. Senoo et al. [34] recently reported the presence of stellate like cells in the intestine which store vitamin A. It is possible these strongly immunoreactive cells are an extrahepatic intestinal stellate cell that stores vitamin A and carotenoids. Although the majority of vitamin A is stored in stellate cells of the liver, extrahepatic storage also exists in stellate cells of various tissues such as pancreas [35], lung, kidney, intestine [36] and vocal folds [37]. Intestinal epithelial function is severely compromised in vitamin A deficiency. Storage of vitamin A directly in tissues with high need allows for an emergency backup in times of deficiency.

Another highly immunoreactive area for BCO1 was the Brunner's glands in the duodenum [38]. These glands, which are largely found in the submucosa of the proximal duodenum secrete copious mucin glycoproteins thought to form a protective barrier for the mucosal surface [39,40]. They also secrete other factors such as ions, water, and both proteins and lipids. The presence of BCO1 in Brunner's glands is a curious finding indicating exocrine secretions from these glands may initiate the process of carotenoid digestion. BCO1 action in the duodenum could lead to rapid uptake of retinal by absorptive cells.

BCO2 expression in the small intestine occurred along the epithelial cells of the villi as well as in endothelial cells. In addition BCO2 was expressed in the submucosa and muscularis of the small intestine in agreement with its presence in skeletal muscle [25]. Finally, small, strongly immunoreactive cells similar to those found to express BCO1 were also present along the villi and Peyer's patches. Because Peyer's patches are part of the gut associated lymphoid tissue the presence of BCO2 indicates possible activity in immune function. It is possible that these strongly immunolocalized cells are intestinal stellate cells since their presence and distribution were similar to those described by Senoo et al. [34].

Acknowledgments

The authors gratefully acknowledge support from the National Institutes of Health through research grants R01-DK044498 (EHH), R01-HL049879 (EHH), R01-DK068437 (WSB) and the services of Veterinary Histology

Laboratory, The Ohio State University (Columbus, OH, USA). We also thank Dr. Helen Everts for the use of her Olympus BX51 light microscope.

References

1. Ross, AC.; Harrison, EH. Handbook of Vitamins. 5th ed.. Zempleni, J.; Suttie, JW.; Gregory, JF., III; Stover, PJ., editors. CRC Press; 2014. p. 1-49.
2. Gudas LJ. Biochim. Biophys. Acta. 2012; 1821:213–221. [PubMed: 21855651]
3. Saari JC. Annu. Rev. Nutr. 2012; 32:125–145. [PubMed: 22809103]
4. Balmer JE, Blomhoff R. J. Lipid Res. 2002; 43:1773–1808. [PubMed: 12401878]
5. Chambon P. FASEB J. 1996; 10:940–954. [PubMed: 8801176]
6. Sommer A. Prog. Retin. Eye Res. 1998; 17:9–31. [PubMed: 9537797]
7. Theodosiou M, Laudet V, Schubert M. Cell. Mol. Life Sci. 2010; 67:1423–1445. [PubMed: 20140749]
8. During A, Harrison EH. Arch. Biochem. Biophys. 2004; 430:77–88. [PubMed: 15325914]
9. Harrison EH. Biochim. Biophys. Acta. 2012; 1821:70–77. [PubMed: 21718801]
10. U.S. Institute of Medicine, Food and Nutrition Board. Dietary Reference Intakes for Vitamin A, Vitamin K, Arsenic, Boron, Chromium, Copper, Iodine, Iron, Manganese, Molybdenum, Nickel, Silicon, Vanadium, and Zinc. Washington: National Academy Press; 2002.
11. Bendich A, Olson JA. FASEB J. 1989; 3:1927–1932. [PubMed: 2656356]
12. Lindqvist A, Andersson S. J. Biol. Chem. 2002; 277:23942–23948. [PubMed: 11960992]
13. During A, Nagao A, Hoshino C, Terao J. Anal. Biochem. 1996; 241:199–205. [PubMed: 8921188]
14. Paik J, During A, Harrison EH, Mendelsohn CL, Lai K, Blaner WS. J. Biol. Chem. 2001; 276:32160–32168. [PubMed: 11418584]
15. Redmond TM, Gentleman S, Duncan T, Yu S, Wiggert B, Gantt E, Cunningham FX Jr. J. Biol. Chem. 2001; 276:6560–6565. [PubMed: 11092891]
16. Wyss A, Wirtz G, Woggon W, Brugger R, Wyss M, Friedlein A, Bachmann H, Hunziker W. Biochem. Biophys. Res. Commun. 2000; 271:334–336. [PubMed: 10799297]
17. Kiefer C, Hessel S, Lampert JM, Vogt K, Lederer MO, Breithaupt DE, von Lintig J. J. Biol. Chem. 2001; 276:14110–14116. [PubMed: 11278918]
18. O'Byrne SM, Blaner WS. J. Lipid Res. 2013; 54:1731–1743. [PubMed: 23625372]
19. Martucci RB, Ziulkoski AL, Fortuna VA, Guaragna RM, Guma FC, Trugo LC, Borojevic R. J. Cell. Biochem. 2004; 92:414–423. [PubMed: 15108365]
20. Shmarakov I, Fleshman MK, D'Ambrosio DN, Piantedosi R, Riedl KM, Schwartz SJ, Curley RW Jr, von Lintig J, Rubin LP, Harrison EH, Blaner WS. Arch. Biochem. Biophys. 2010; 504:3–10. [PubMed: 20470748]
21. Teodoro AJ, Perrone D, Martucci RB, Borojevic R. Eur. J. Nutr. 2009; 48:261–268. [PubMed: 19533199]
22. Amengual J, Lobo GP, Golczak M, Li HN, Klimova T, Hoppel CL, Wyss A, Palczewski K. J. von Lintig, FASEB J. 2011; 25:948–959.
23. Hessel S, Eichinger A, Isken A, Amengual J, Hunzelmann S, Hoeller U, Elste V, Hunziker W, Goralczyk R, Oberhauser V, von Lintig J, Wyss A. J. Biol. Chem. 2007; 282:33553–33561. [PubMed: 17855355]
24. Lindqvist A, Andersson S. J. Histochem. Cytochem. 2004; 52:491–499. [PubMed: 15034000]
25. Lindqvist A, He YG, Andersson S, Histochem J. Cytochem. 2005; 53:1403–1412.
26. Palczewski G, Amengual J, Hoppel CL. J. von Lintig, FASEB J. 2014; 28:4457–4469.
27. Harrison EH, Blaner WS, Goodman DS, Ross AC. J. Lipid Res. 1987; 28:973–981. [PubMed: 3668391]
28. Grune T, Lietz G, Palou A, Ross AC, Stahl W, Tang G, Thurnham D, Yin SA, Biesalski HK. J. Nutr. 2010; 140:2268S–2285S. [PubMed: 20980645]
29. Shmarakov IO, Jiang H, Yang KJ, Goldberg IJ, Blaner WS. J. Lipid Res. 2013; 54:893–908. [PubMed: 23349206]

30. Nagatsuma K, Hayashi Y, Hano H, Sagara H, Murakami K, Saito M, Masaki T, Lu T, Tanaka M, Enzan H, Aizawa Y, Tajiri H, Matsuura T. Liver Int. 2009; 29:47–54. [PubMed: 18544127]
31. Wyss A, Wirtz GM, Woggon WD, Brugger R, Wyss M, Friedlein A, Riss G, Bachmann H, Hunziker W. Biochem. J. 2001; 354:521–529. [PubMed: 11237856]
32. Wake K. J. Electron. Microsc. (Tokyo). 1999; 48:89–98. [PubMed: 10356785]
33. Bohnsack BL, Lai L, Dolle P, Hirschi KK. Genes Dev. 2004; 18(11):1345–1358. [PubMed: 15175265]
34. Senoo H, Mezaki Y, Morii M, Hebiguchi T, Miura M, Imai K. Cell Biol. Int. 2013; 37:1171–1180. [PubMed: 23765517]
35. Apte MV, Pirola RC, Wilson JS. Front. Physiol. 2012; 3:344. [PubMed: 22973234]
36. Nagy NE, Holven KB, Roos N, Senoo H. J. Lipid Res. 1997; 38:645–658. [PubMed: 9144080]
37. Sato K, Umeno H, Nakashima T. Ann. Otol. Rhinol. Laryngol. 2012; 2012(121):51–56. [PubMed: 22312928]
38. Friend DS. J. Cell Biol. 1965; 25:563–576. [PubMed: 5839256]
39. Krause WJ. Prog. Histochem. Cytochem. 2000; 35:259–367. [PubMed: 11148980]
40. Collaco AM, Jakab RL, Hoekstra NE, Mitchell KA, Brooks A, Ameen NA. Am. J. Physiol. Gastrointest. Liver Physiol. 2013; 305:G258–G275. [PubMed: 23744739]

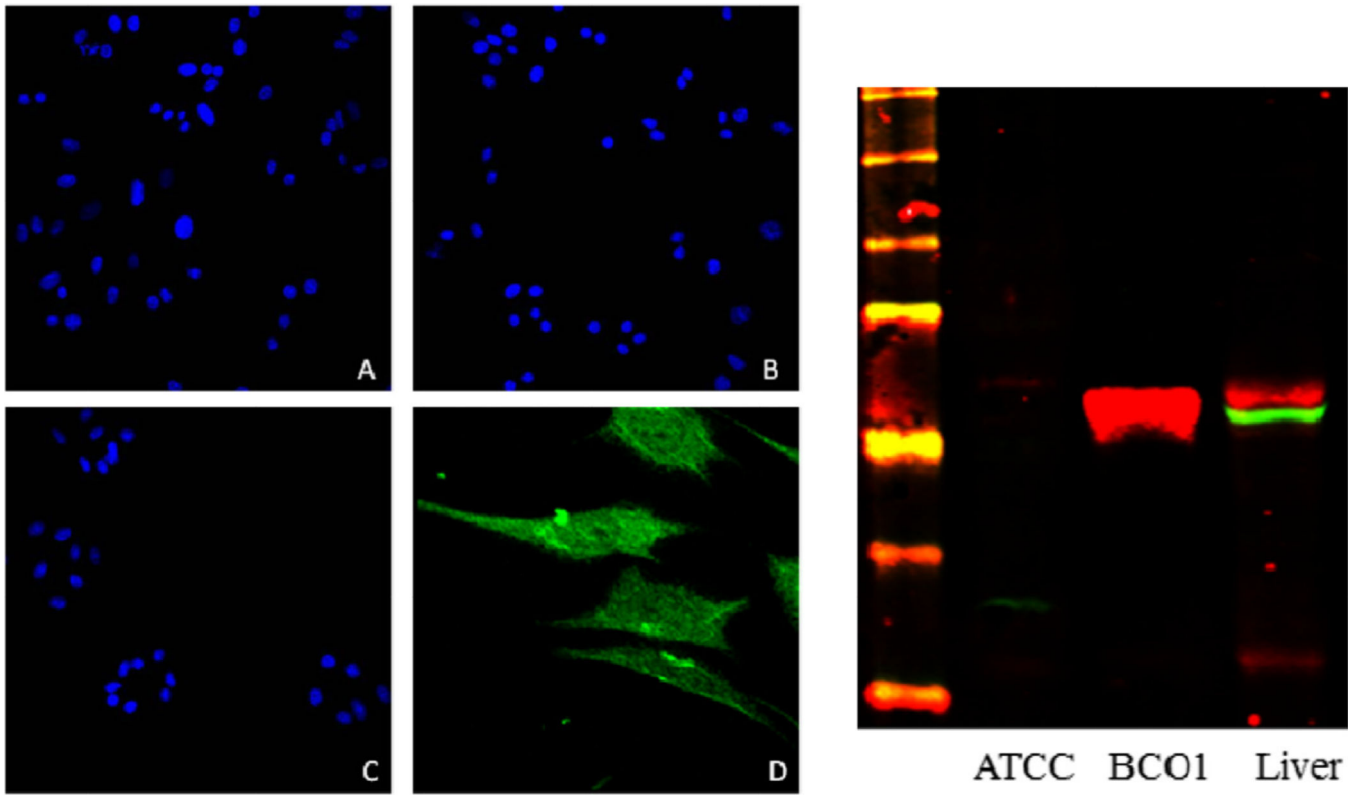

Fig. 1.

Immunoblots showing specificity of BCO1 and BCO2 antibodies. The specificity of antibody to BCO1 (1:5000) was verified by immunofluorescence. Cell nuclei are stained blue with DAPI. ATCC CHO cells are negative for (A) BCO1 and (B) BCO2. (C) BCO2 (1:5000) antibody shows no immunoreactivity in BCO1 cDNA transfected cell line (NY CHO). (D) NY CHO cells stably transfected with BCO1 show positive immunoreactivity (Alexa 488) with BCO1 antibody. Images obtained with the Olympus FV1000 confocal microscope. Specificity of antibodies was also verified with Western blot (gel on right). BCO1 shows immunoreactivity at ~63 kDa in BCO1 cDNA transfected cell line (BCO1) and whole liver homogenate (LIVER) as a red band, but no reactivity in ATCC-CHO cells. BCO2 show immunoreactivity at ~60 kDa in whole liver homogenate as a green band, but no reactivity with ATCC-CHO or BCO1-CHO cells. Molecular weight markers shown at left. Total protein per well was 40 μg.

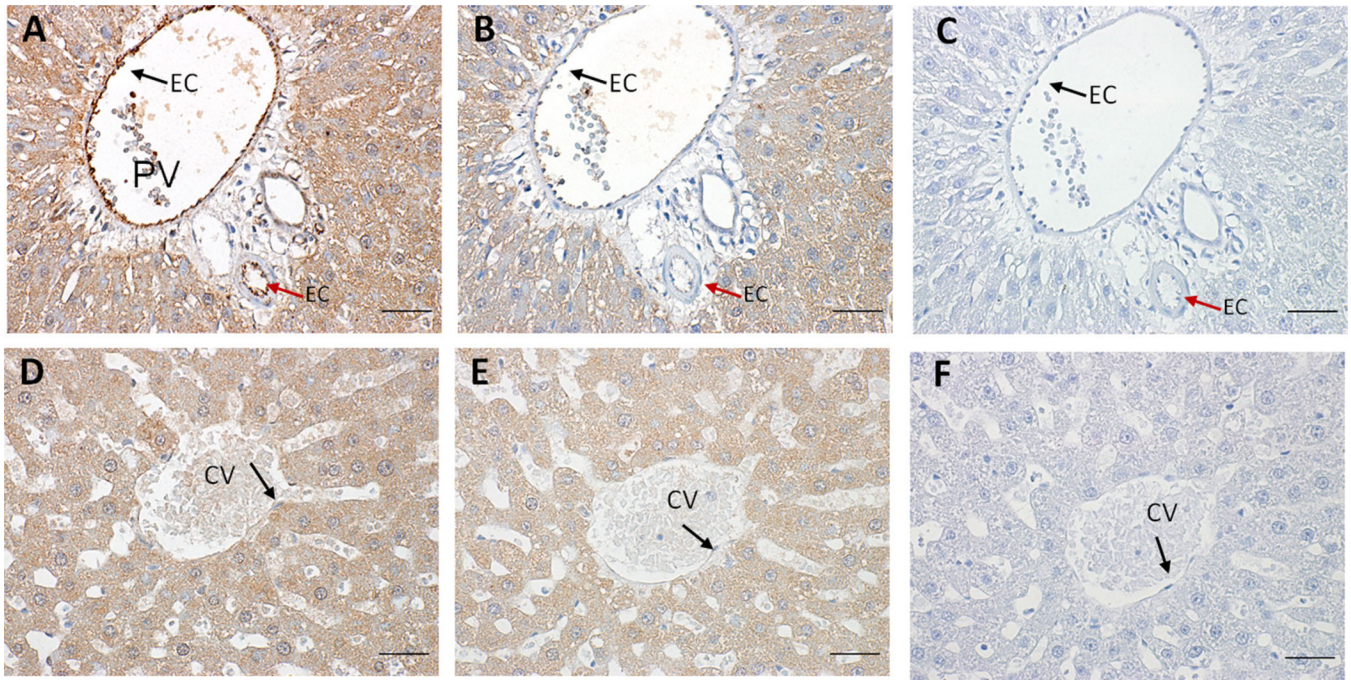

Fig. 2.

Comparison of BCO1 and BCO2 protein expression in serial sections of rat liver tissue. Specific staining shown in brown. (A) Localization of BCO1 (1:250) in endothelial cells lining portal vein (black arrow, EC) and hepatic artery (red arrow, EC). (B) BCO2 (1:250) protein expressed in peri-portal hepatocytes. Portal endothelial cells (EC) lack BCO2 expression. Endothelial cells of central vein is negative for BCO1 and BCO2 (arrows, panel D–E). Panel C and F are negative controls for BCO1 and BCO2. PV, portal vein EC, endothelial cells, CV, central vein, scale bar = 35 μm.

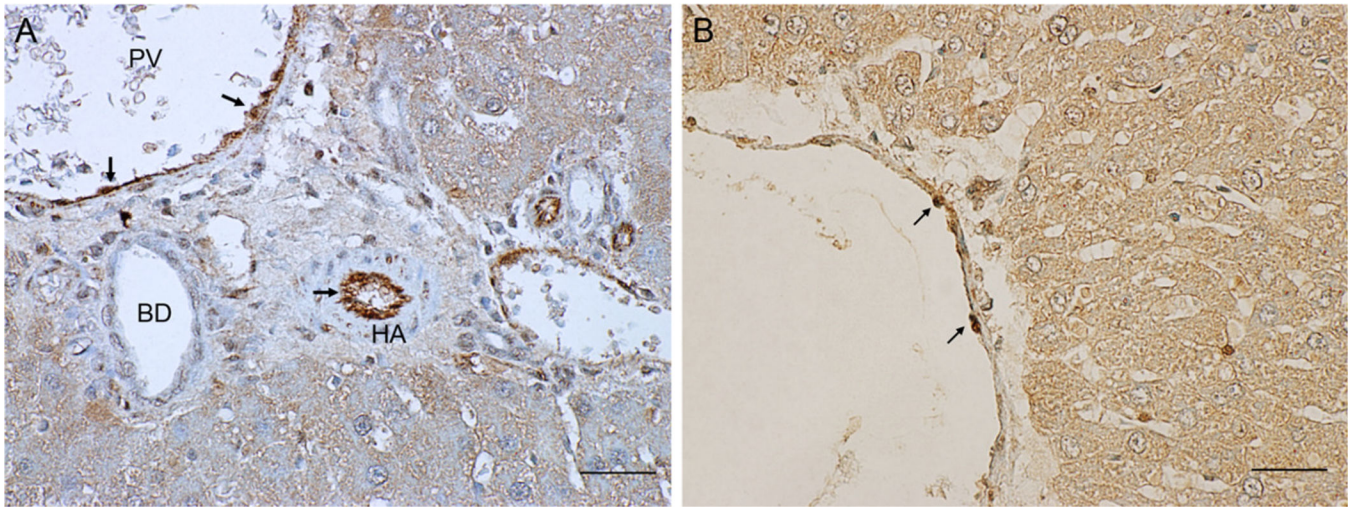

Fig. 3.

Expression and localization of BCO1 in endothelial cells. (A) Arrows indicate the endothelial cells of HA and PV that are positively stained for BCO1 (1:250). Note that endothelial cells lining bile duct are negative for BCO1. (B) Higher magnification of portal vein endothelial cells shows BCO1 staining. PV, portal vein; BD, bile duct; HA, hepatic artery. Scale bar 40 μm.

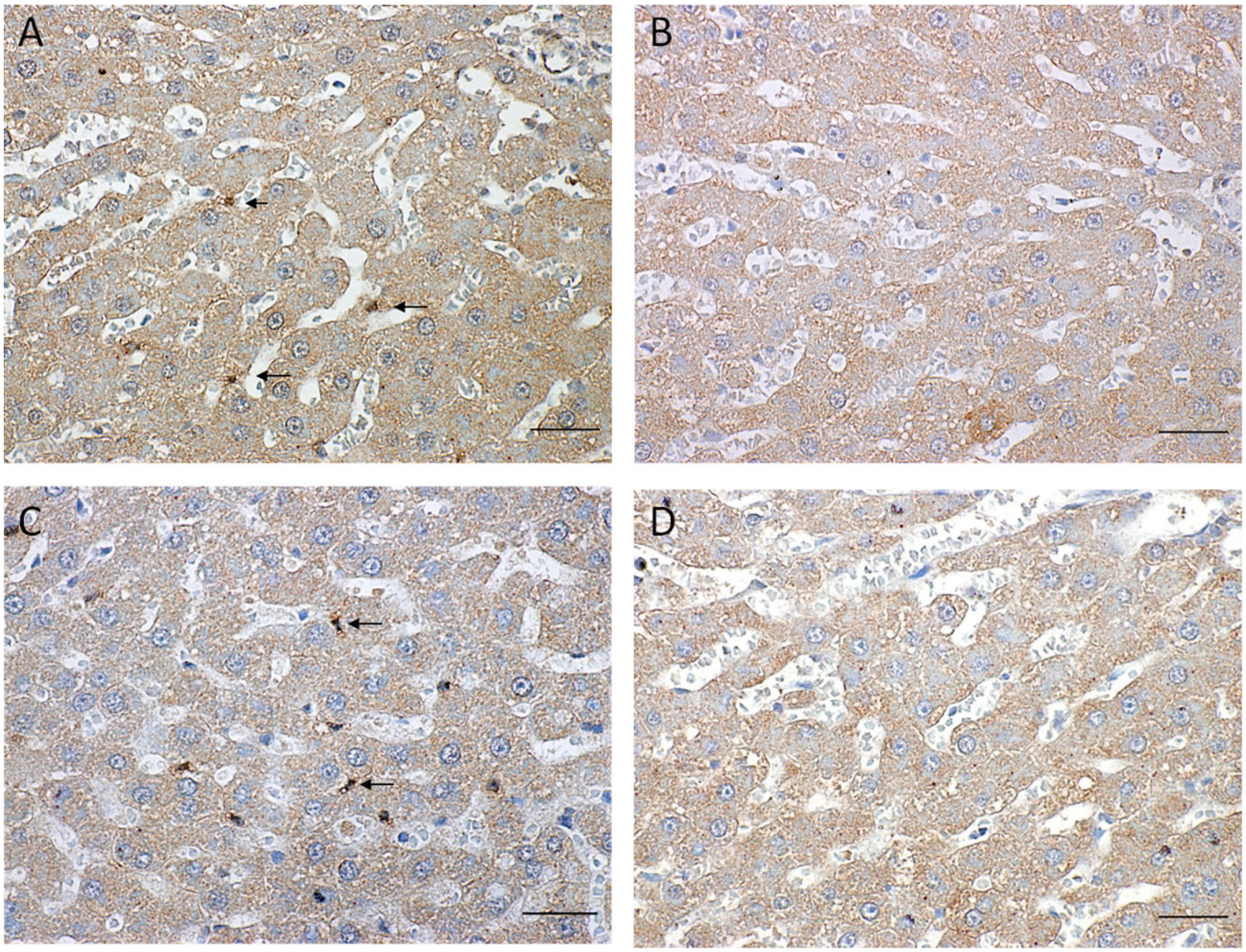

Fig. 4.

Comparison of BCO1 and BCO2 protein expression in parenchyma. Panel A and C shows localization of BCO1 (1:250) protein in parenchyma. Hepatic stellate cells shows BCO1 expression in parenchyma (A and C, arrows). Panel B and D shows BCO2 expression in parenchyma. Scale bar = 35 μm.

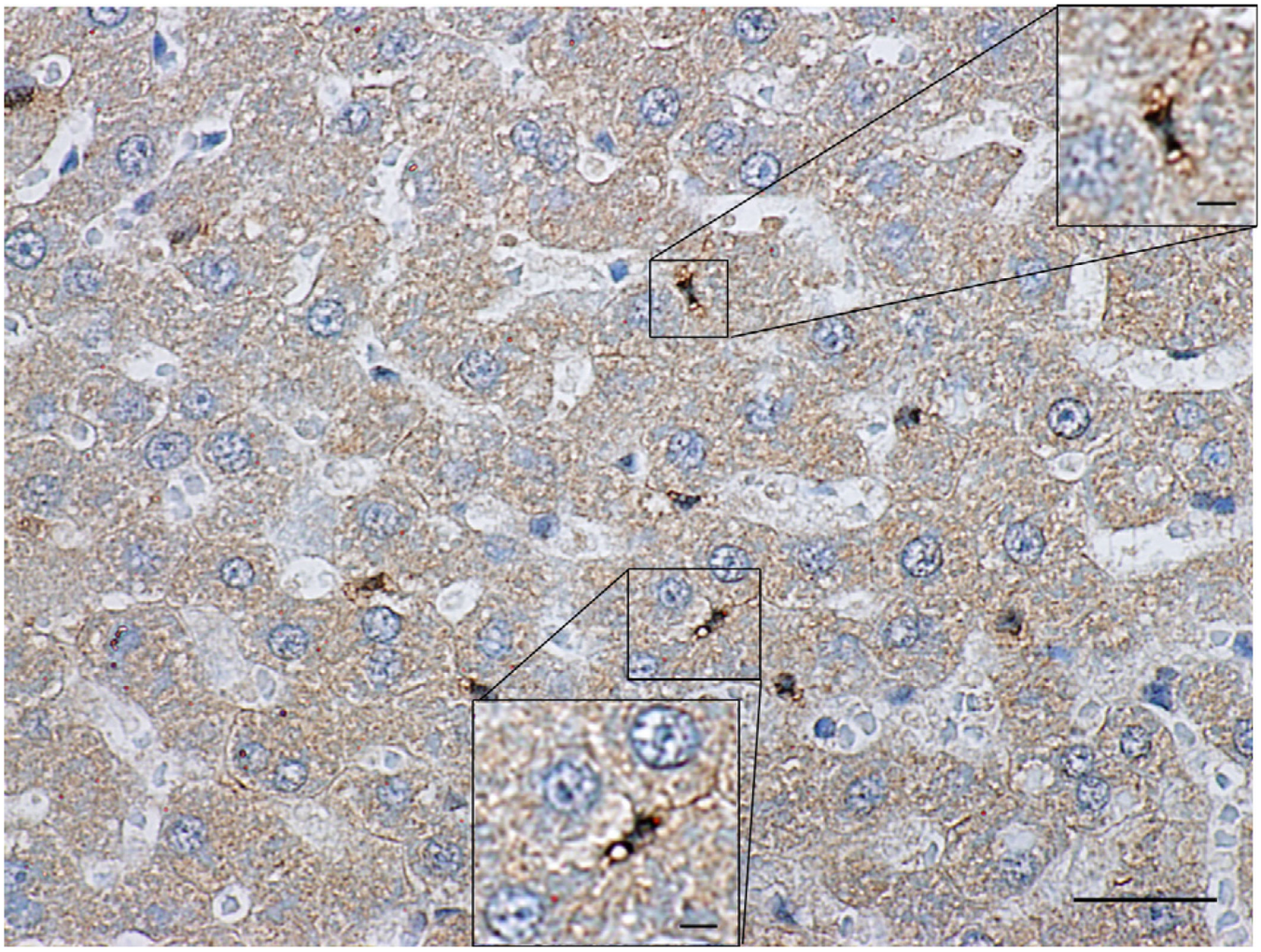

Fig. 5.

Expression of BCO1 protein in hepatic stellate cells. BCO1 (1:250) uniformly expressed in hepatocytes (brown presence with blue nucleus). Hepatic stellate cells (HSC) with lipid droplets, shown at higher magnification (in insets), also shows strong reactivity for BCO1 antibody. Scale bar 35 μm, 7 μm (inset).

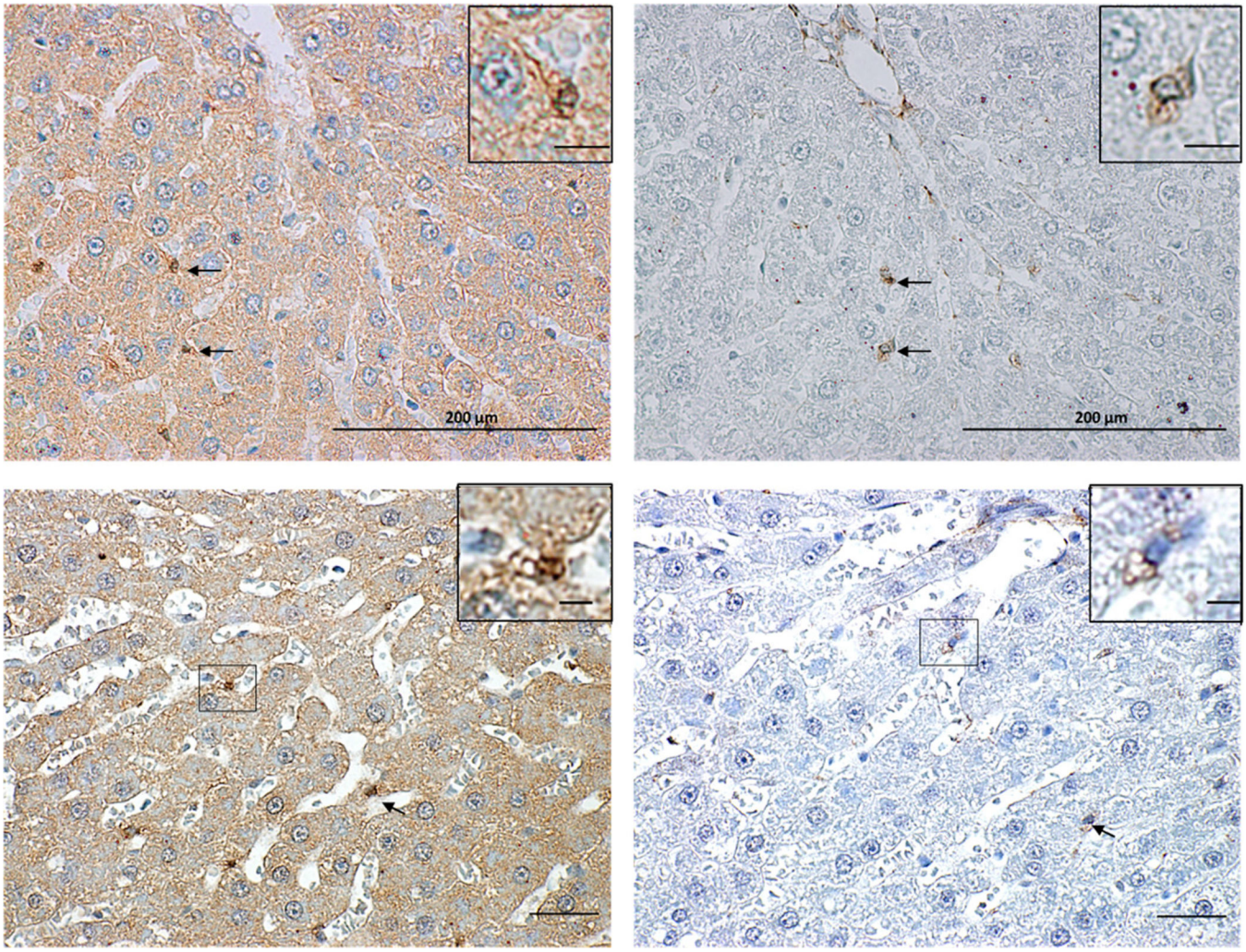

Fig. 6.

Expression of BCO1 and desmin (stellate cell marker) in serial sections of rat liver. Arrows shows HSC immunostained with BCO1 (1:250) antibody (left panels) co-localize with the HSC stained for desmin (1:50; DES, right panels). Insets denote the HSC immunostained for BCO1 and desmin at higher magnification. Scale bar 35 μm, insets, 7 μm.

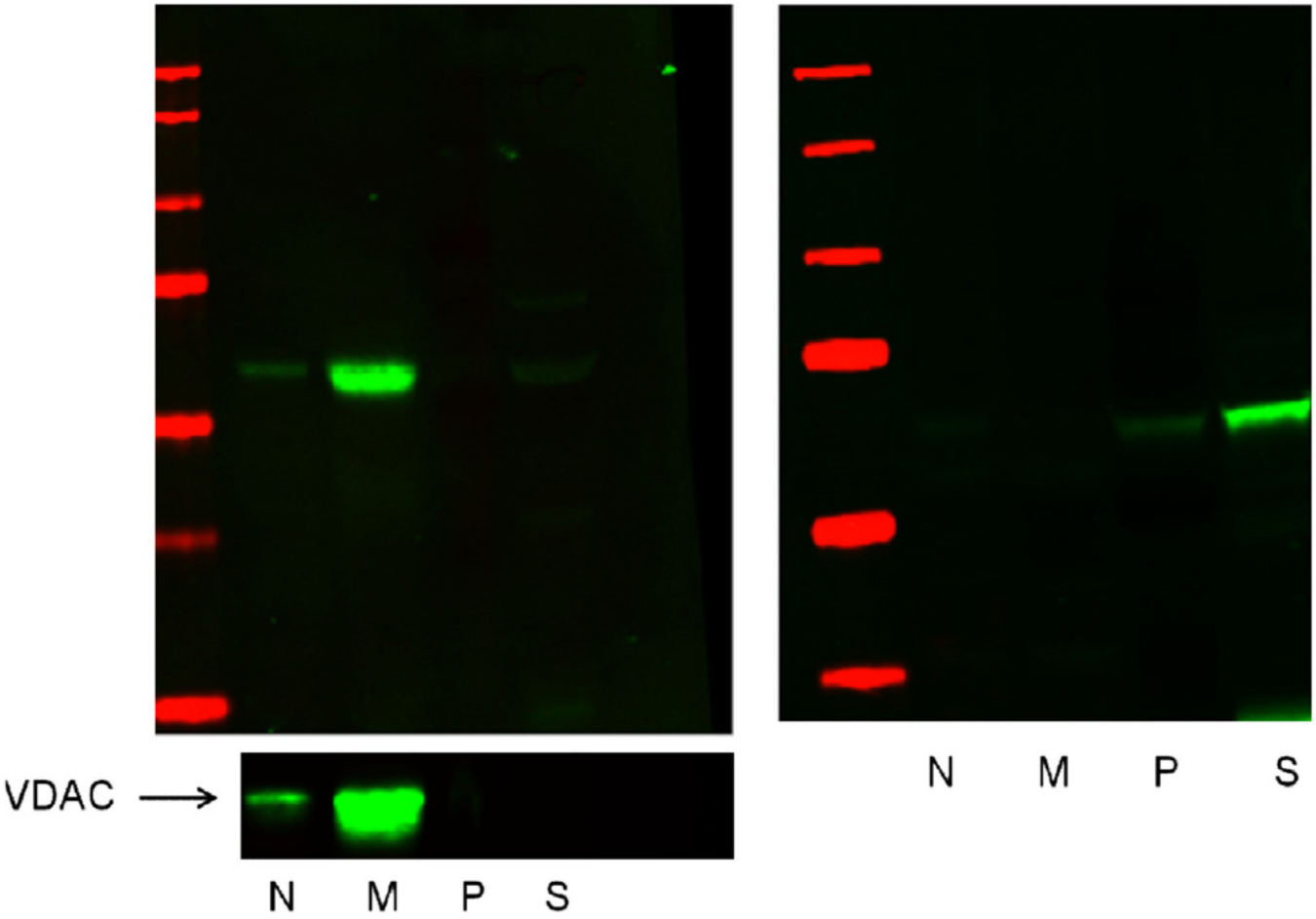

Fig. 7.

Immunoblots showing sub-cellular expression of BCO1 (1:5000), BCO2 (1:5000) and VDAC1 (1:2000) proteins in rat liver cell fractions including nuclear (N), mitochondrial (M), microsomal (P) and cytosolic (S). Left panels show the expression of BCO2 (full gel) and VDAC1 (lower gel) in liver cell fractions. Right panel shows the expression of BCO1 in the same fractions. Equal quantities of total protein were loaded on each lane.

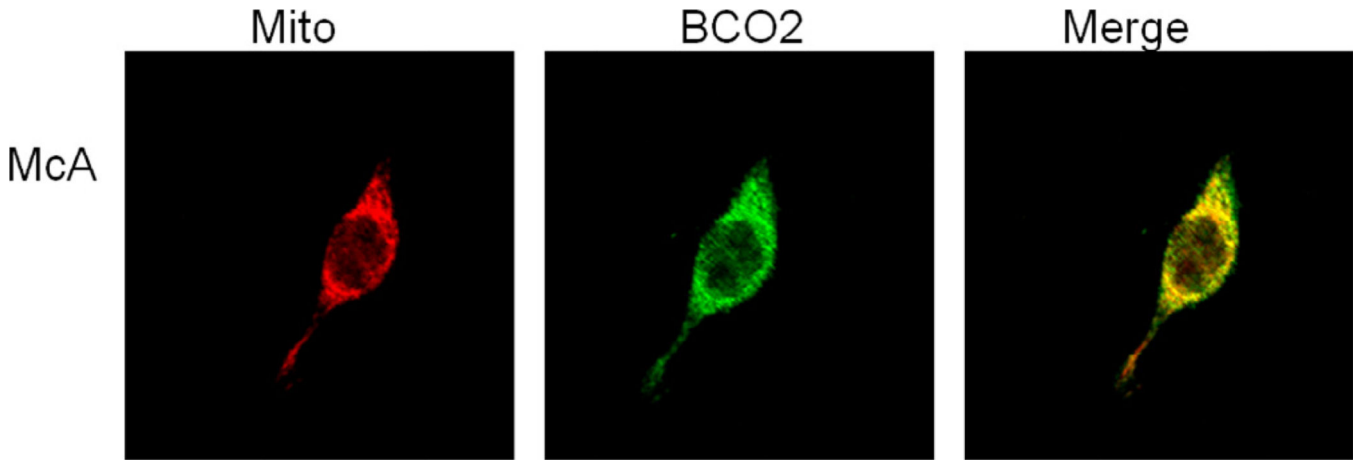

Fig. 8.

Co-localization of BCO2 and mitotracker. Double immunofluorescence staining shows for BCO2 (1:2000) (green) and 400 nM mitotracker (red) in McA cells. Right panel shows merged image for mitotracker dye and endogenously expressed BCO2 protein in McA cells. Yellow color shows colocalization of BCO2 with mitotracker. Images were obtained using confocal microscope with × 40 objective.

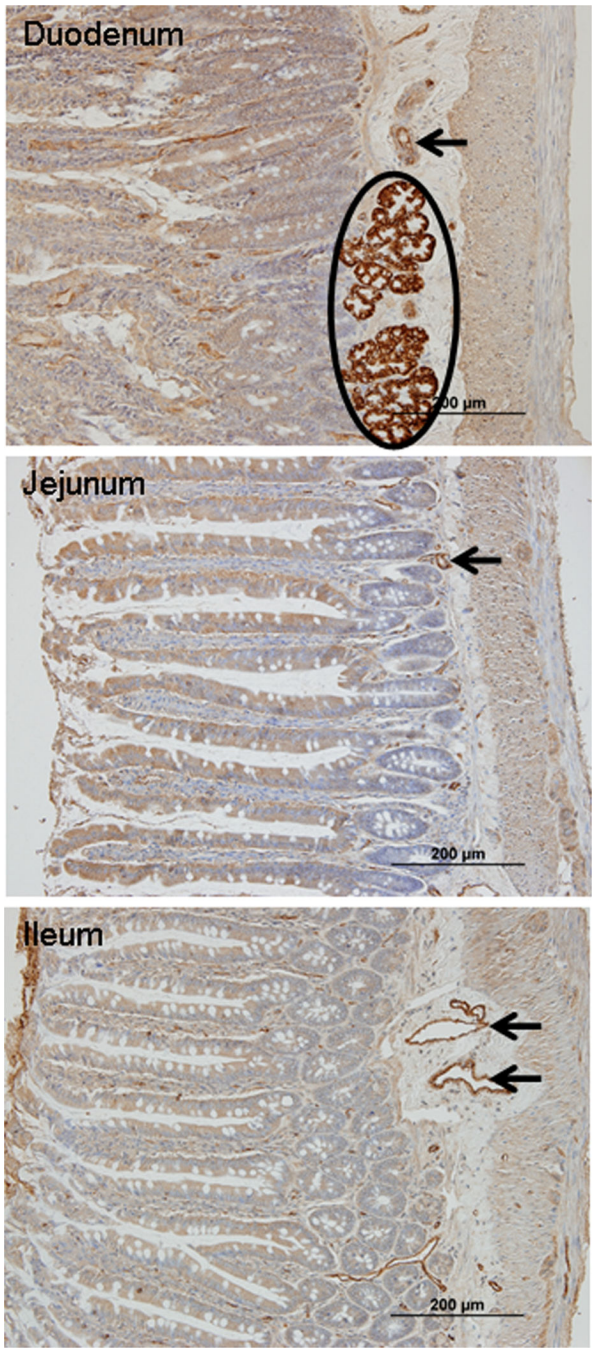

Fig. 9.

BCO1 immunoreactivity in intestinal sections. Strongest immunoreactivity in duodenum (antibody dilution 1:1000) (A) with less reactivity in jejunum (B) and ileum (C) (antibody dilution 1:500). Villus, crypt, and muscular cells show diffuse presence. Strong presence in Brunner's glands (circled) and endothelial cells (arrows).

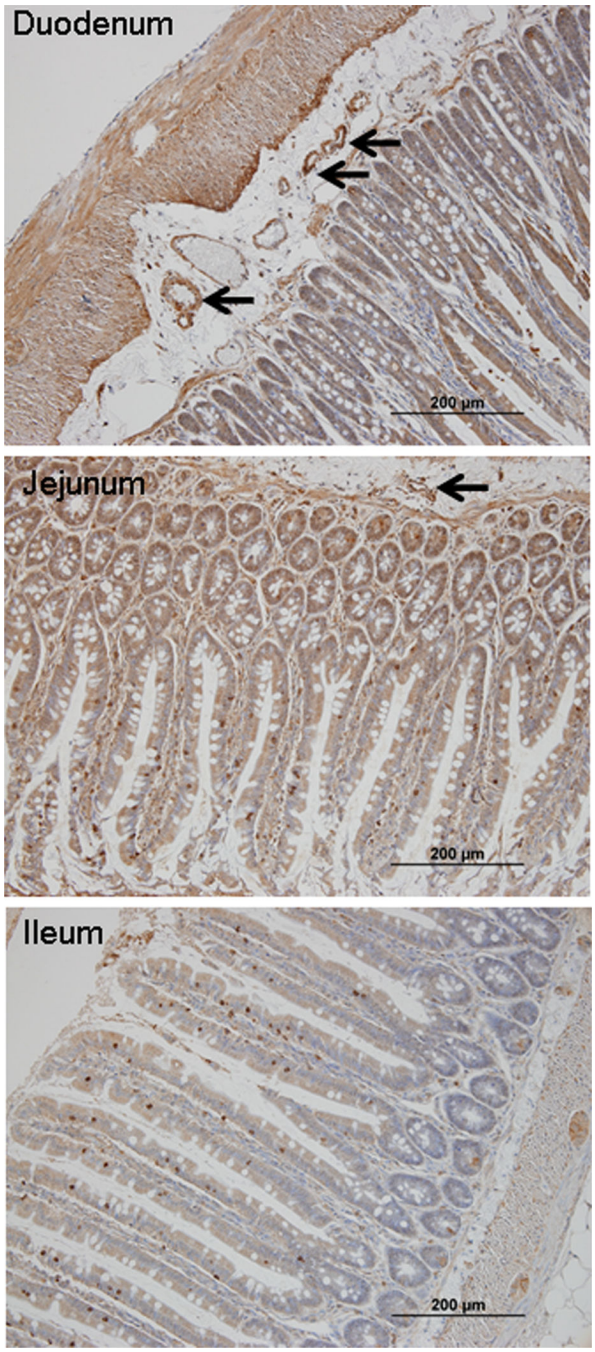

Fig. 10.

BCO2 immunoreactivity in intestinal sections. Strongest immunoreactivity of BCO2 (1:750) in duodenum (A) with less reactivity in jejunum (B) and ileum (C). Diffuse pattern in villi, crypt, and muscle cells. Strong reactivity in endothelial cells (arrows).

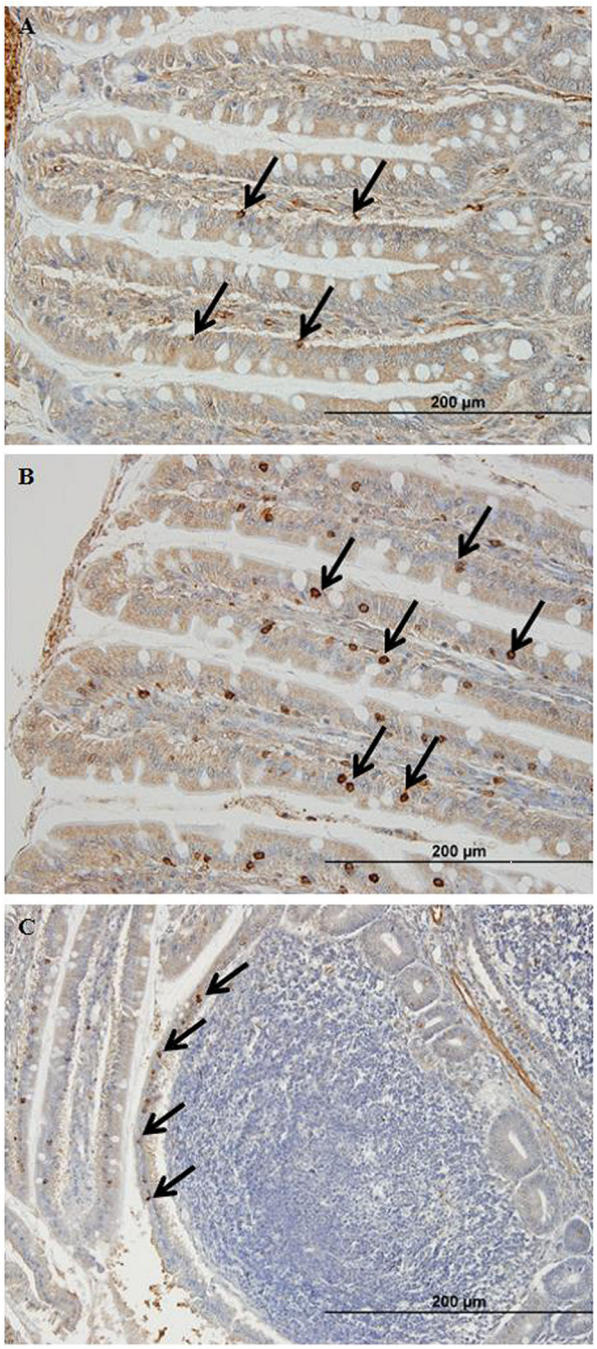

Fig. 11.

Immunoreactivity of BCO1 and BCO2 in specific epithelial cells in the small intestine. Strong, punctuate presence in specific epithelial cells (arrows) along villi with BCO1 (1:500; A). BCO2 (1:500) presence in a strong punctuate pattern in specific epithelial cells (arrows) along villi (B). BCO2 presence in a strong punctuate pattern in specific cells (arrows) along Peyer's patches (C).